Available online at www.sciencedirect.com
SCIENCE DIRECT®
Journal of Solid State Chemistry 177 (2004) 2920–2927
JOURNAL OF SOLID STATE CHEMISTRY
http://elsevier.com/locate/jssc

Reaction of $SbPO_4$ with lithium in non-aqueous electrochemical cells: preliminary study and evaluation of its electrochemical performance in anodes for lithium ion batteries

J. Santos Peña,[a,*] J. Cuart Pascual,[a] A. Caballero,[b] J. Morales,[b] and L. Sánchez[b]

[a] *Departament de Química, Universitat de les Illes Balears, Edifici Mateu Orfila i Rotger, Cra. de Valldemosa, km. 7.5, 07123 Palma, Spain*
[b] *Departamento de Química Inorgánica e Ingeniería Química, Edificio Marie Curie, Campus de Rabanales, Universidad de Córdoba, 14071 Córdoba, Spain*

Received 20 February 2004; received in revised form 27 April 2004; accepted 28 April 2004

Abstract

$SbPO_4$, a phosphate with a layered structure, was tested as an electrode material for lithium cells spanning the 3.0–0.0 V range. Two main electrochemical processes were detected as extensive plateaus at ca. 1.6 and 0.7 V in galvanostatic measurements. The first process was found to be irreversible, thus excluding a potential intercalation-like mechanism for the reaction and being better interpreted as a decomposition reaction leading to the formation of elemental Sb. This precludes the use of this compound as a cathodic material for lithium cells. By contrast, the process at 0.7 V is reversible and can be ascribed to the formation of lithium–antimony alloys. The best electrochemical response was obtained by cycling the cell at a $C/20$ discharge rate over the voltage range 1.25–0.25 V. Under these conditions, the cell delivers an average capacity of 165 Ah/kg—a value greater than those reported for other phosphates—upon successive cycling.

Keywords: Antimony orthophosphate; Negative electrodes; Lithium ion batteries; Lithium–antimony alloys

1. Introduction

Layered inorganic compounds possess interesting properties as electrode materials for lithium ion batteries. Thus, the interlayer spacing provides interstitial positions for lithium ions to be accommodated following a topotactic reaction which justifies the good cyclability exhibited by some systems. Upon intercalation, lithium can diffuse through interstitial sites via a jumping mechanism subject to relatively low energy barriers; this results in efficient diffusion, which is a desirable feature in high-rate rechargeable batteries. So far, transition metal layered oxides, $LiMO_2$ (M = Co, Ni, Mn), have exhibited the best electrochemical response as cathodic materials in lithium cells [1–4].

Except for graphite-based carbons, there appears to be no reference to the use of layered systems with electrochemically intercalated lithium as negative electrodes. Since the early 1990s, however, there has been an increasing interest in negative electrodes based on metal oxides, the reaction of which with lithium involves the reduction of the oxide to metal particles in the electrode. The most promising electrodes in this context are tin oxides. Further reaction between lithium and in situ formed tin accounts for the reversible electrochemical formation of Li_xSn alloys ($1.0 < x < 4.4$) and is the origin of its electrochemical performance [5,6]. Recently, some layered metallic phosphates such as SnP_2O_7 [7], $SnHPO_4$ [8] and $Pb_3(PO_4)_2$ [9] have been proposed as precursors of the negative electrode for lithium ion batteries. The mechanism of the reaction between lithium and these compounds is not consistent with an intercalation process where lithium would occupy the interstices between the layers defined by M–PO_4 units [M denoting Sn(II) or Pb(II)]. This is fairly unsurprising as the intercalation process should promote the reduction of M(II) and a subsequent decrease in M–O binding

*Corresponding author. Fax: +34-971173426.
E-mail address: vdqujsp@uib.es (J. Santos Peña).

0022-4596/$ - see front matter © 2004 Published by Elsevier Inc.
doi:10.1016/j.jssc.2004.04.050

energy, which destabilizes the structure. The basic scheme of the reaction of lithium with other tin/lead salts or oxides involves the formation of metallic atoms and a lithium compound [5,6,10,11]. Liu et al. have suggested that the reaction with lithium destroys the $Pb_3(PO_4)_2$ structure and results in the formation of lithium phosphate and lead particles in the electrode, according to

$$Pb_3(PO_4)_2 + 6\ Li^+ + 6\ e^- \rightarrow 3\ Pb + 2\ Li_3PO_4 \quad (1)$$

This reaction is interesting with a view to obtain negative electrode materials as in situ formed metallic particles can react reversibly with lithium to form the $Li_{4.4}Pb$ alloy [10,11] (or the $Li_{22}Sn_5$ alloy [12,13] with tin phosphate) at a potential close to 0.0 V. However, the capacity of these phosphates has been shown to decline after a few cycles. Such a capacity loss can be ascribed to the formation of large lead or tin clusters during cycling that reduce the percolation paths associated to electron and lithium diffusion [14].

Structurally, $SbPO_4$ consists of sheets of PO_4 tetrahedra and SbO_4 polyhedra connected through the corners thereby forming an extended network. Infinite sheets of $SbPO_4$ composition are then stacked in the direction of the *a*-axis [15]. This compound has the ability to intercalate various organic molecules while retaining its layered framework [16]. In this work, we studied the reactivity of this compound towards lithium in non-aqueous electrochemical cells. We have considered two different voltage ranges for operating with positive and negative electrodes, and examined the different states of discharge of the electrode by using various techniques with the aim of elucidating the mechanism of the reaction between lithium and the phosphate. Also, we evaluated the electrochemical performance of the cell in terms of current density and potential range.

2. Experimental

Antimony orthophosphate was freshly prepared as reported elsewhere [17] by treating antimony oxide (valentinite polymorph) in a 6 M H_3PO_4 solution. After three days of stirring at room temperature, a white solid was collected, filtered and washed with excess water in order to remove the phosphorus oxides formed during the obtainment of the orthophosphate. The contents in Sb and PO_4 were determined by digesting a sample with sulfuric acid. Subsequently, Sb(III) was titrated with $KBrO_3$ and PO_4 analyzed as phosphomolybdate by absorption spectrophotometry. As expected, an Sb:PO_4 ratio of 1:1 was obtained.

X-ray diffraction (XRD) patterns were recorded on a Siemens D5000 X-ray diffractometer, using Cu$K\alpha$ radiation and a graphite monochromator. Ex situ X-ray patterns for samples at different states of discharge were obtained by covering the electrode with Mylar film to avoid contact with the atmosphere. Scanning electron microscopy (SEM) images were obtained on a Leica Stereoscan microscope. For SEM examination of the discharge electrodes, samples were previously extensively washed with acetonitryle in order to remove the electrolyte and its solvent. TEM images were obtained with a Hitachi H600 instrument operating at 75 kV.

FTIR spectra were collected with a Bruker IFS66 instrument used in the transmittance mode. Spectra were recorded at 4 cm^{-1} intervals over the 4000–400 cm^{-1} range.

Electrochemical tests were carried out at room temperature, using a simple two-electrode cell with metallic lithium as negative electrode. The electrolyte used was a Merck battery electrolyte LP 40 [ethylene carbonate (EC): diethylcarbonate (DEC) = 1:1 w/w, 1 M $LiPF_6$]. Electrode pellets (7 mm in diameter) were prepared by pressing, in an stainless-steel grid, ca. 4 mg of active material with polytetrafluoroethylene (PTFE) (5 wt%), and acetylene black (20 wt%) at 4 ton. Lithium foil was cut into circles 7 mm in diameter.

Cyclic voltammetry (CV) tests were performed at a scan rate of 50 $\mu V\,s^{-1}$, using a Schlumberger SI-1286 potentiostat. Galvanostatic tests were performed with a MacPile II potentiostat–galvanostat (*Biologic*), using different galvanostatic regimes from *C*/5 to *C*/20 (*C* being defined as 1 Li in 1 h).

3. Results and discussion

3.1. Structural characterization

The purity of antimony orthophosphate was checked by recording the corresponding XRD pattern (Fig. 1a), which was consistent with ICDD card No. 35-829. $SbPO_4$ crystallizes in the monoclinic system, space group $P2_1/m$, with the following refined cell parameters: $a = 5.095(3)$ Å, $b = 6.769(2)$ Å, $c = 4.742(8)$ Å, $\beta = 94.53(1)^\circ$, in good agreement with those obtained by Sudarsan et al. [17] Samples were observed by TEM after ultrasonication of a phosphate dispersion in methanol (Fig. 2). As can be seen, $SbPO_4$ particles crystallized as platelets with well-defined edges.

The conversion of valentinite to $SbPO_4$ was checked by infrared measurements. Valentinite bands (688, 586, 552 and 438 cm^{-1}) disappeared after 3 days of treatment with phosphoric acid. The frequencies of the three non-degenerate P–O stretching bands (1137, 1051 and 977 cm^{-1}) and Sb–O vibrations (642 and 590 cm^{-1}) corresponding to P–O–Sb^{+3} linkages were consistent with those reported for orthophosphates [17–19]. The contribution of the O–P–O bending at ca. 600 cm^{-1}

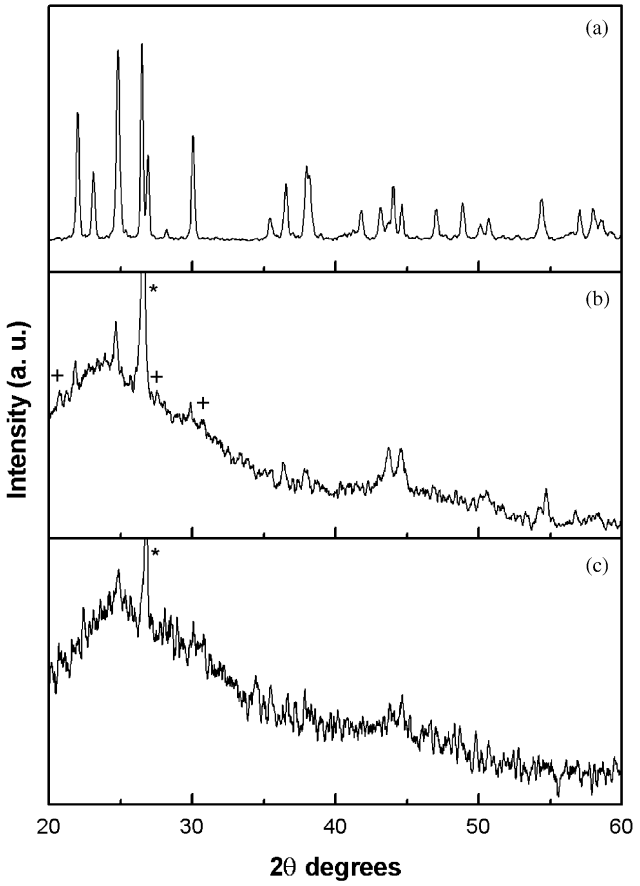

Fig. 1. XRD patterns for pristine $SbPO_4$ (a) and upon subjection to variable discharge depths: $x = 3.0$ (b) and $x = 6.5$ (c) [+ Li_3PO_4; * acetylene black].

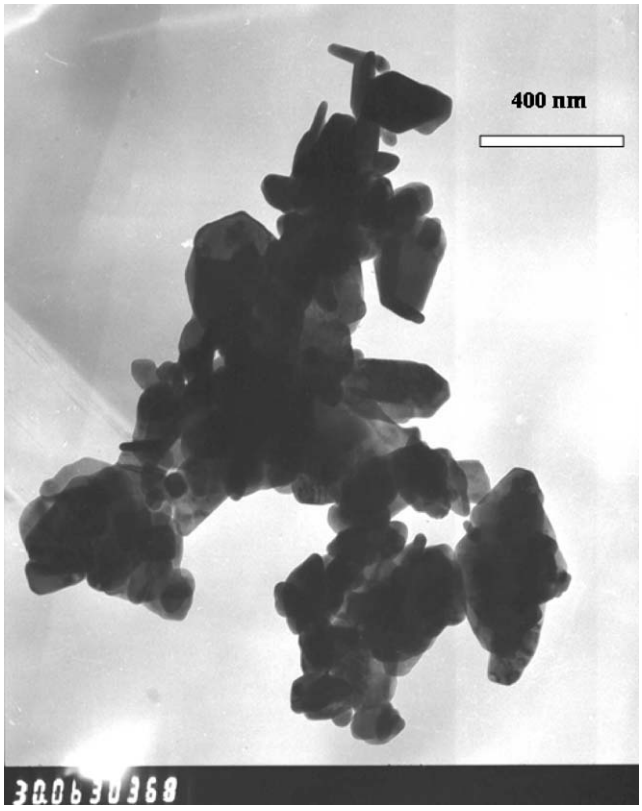

Fig. 2. Transmission electron micrograph of $SbPO_4$.

cannot be ruled out. The contributions of ν(SbO) and $\delta(PO_4)$ gave rise to additional peaks at 499 and 475 cm^{-1}. The absence of bands above 1150 cm^{-1} indicates that no phosphoric acid impurities were trapped in the material during its synthesis.

3.2. Cyclic voltammetry tests

The OCV of the Li/$LiPF_6$(EC, DEC)/$SbPO_4$ cell lay at 3.3 V in all tests. Fig. 3 shows the cyclic voltammograms (CVs) recorded at two different potential ranges compatible with the ability of the material to act as a positive or negative electrode. Over the 2.0–1.2 V range, the cell gave a strong, broad peak centered at 1.32 V in the cathodic wave, but no oxidation peak in the anodic scan. The cyclic voltammograms for crystalline and amorphous lead phosphate electrodes are similar [9], which reflects the irreversibility of the first reduction process in these systems. The experimental curves allow one to discard these phosphates as potential positive electrodes for lithium batteries. More interesting were the results obtained over the 2.0–0.0 V range. Once the first peak at 1.32 V appeared during the discharge

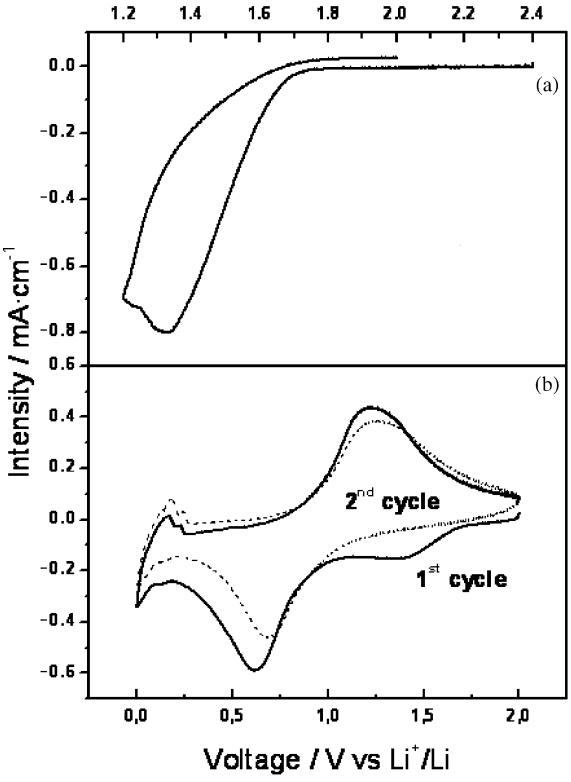

Fig. 3. Cyclic voltammogramms for the Li/$LiPF_6$(EC,DEC)/$SbPO_4$ cell: (a) cycled over the 2.0–1.2 V range, and (b) first and second cycle over the 2.0–0.0 V range.

process, a second peak was observed at 0.7 V, in addition to an anodic peak at 1.27 V. The area of the latter two peaks was similar, which suggests the occurrence of a reversible electrochemical process in this potential range. This evidence was further confirmed by the similarity of these CVs to those obtained in the second cycle and supports the potential use of antimony orthophosphate as a negative electrode. The CVs also exhibited small anodic and cathodic peaks at very low potentials (0.0–0.25 V) that are discussed below.

3.3. Galvanostatic tests

Three different discharge rates ($C/5$, $C/10$ and $C/20$) were used to study the first discharge curve for the $Li/LiPF_6$ (EC, DEC)/$SbPO_4$ cell. As can be seen in Fig. 4, after a first potential decay, the curve exhibited two plateaus at 1.65 and 0.75 V consistent with the two electrochemical processes observed for the first cathodic wave in the CV tests. Interestingly, the reduction processes observed in the galvanostatic occurred at higher potentials than those at the CVs, this can be attributed to the differential kinetics associated to the two techniques. However, the potentials for the plateaus were exactly the same for the three discharge rates, viz. 1.65 and 0.75 V, respectively. After the second plateau, the potential gradually faded to 0.0 V. The characteristics of the plateaus for the different discharge regimes used are shown in Table 1. The current had little influence on the width of the first plateau and the greatest differences were observed in the second electrochemical process. The capacity values associated to the full discharge in the different tests were 594, 717 and 864 A h kg^{-1} for the $C/5$, $C/10$ and $C/20$ discharge regime, respectively. These values are much higher than those exhibited by graphite and justify the study of the reaction of lithium with antimony orthophosphate.

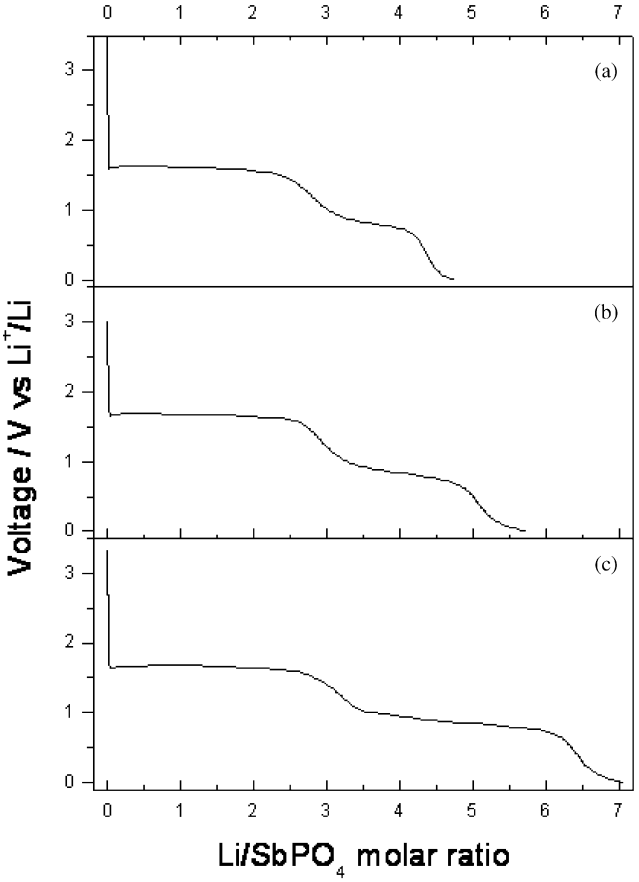

Fig. 4. First galvanostatic discharge of the $Li/LiPF_6$(EC, DEC)/$SbPO_4$ cell under various discharge regimes: (a) $C/5$, (b) $C/10$ and (c) $C/20$.

The potential for the first reduction step, 1.65 V, can be related to that reported for other antimony-based compounds used as negative electrodes in lithium ion batteries [20,21]—except in intermetallic materials. Also, this voltage is similar to that obtained for the reduction of tin (II) phosphates materials [$Sn_3(PO_4)_2$, $Sn_2P_2O_7$ and amorphous Sn_2BPO_6] recently studied by Irvine [7]. The fact that first plateau voltages for the tin derivatives are higher than those reported for tin oxides can be ascribed to the difference in lattice energy of the networks.

According to Li et al., the electrochemical reaction between Sb_2O_3 and lithium takes place at 1.2 V [20] and involves the initial formation of antimony particles:

$$Sb_2O_3 + 6\ Li \rightarrow 2\ Sb + 3\ Li_2O. \quad (2)$$

Recently, Santos-Peña et al. studied the Sb_2O_4 cervantite system [21], the reaction of which with lithium at 1.3 V can be written as:

$$Sb_2O_4 + 8\ Li \rightarrow 2\ Sb + 4\ Li_2O. \quad (3)$$

However, neither (2) nor (3) seems to develop to completion. Moreover, there is a lack of information about Sb–O systems, so amorphous $Li_xSb_2O_3$ or $Li_xSb_2O_4$ phases could be the products of the reaction yielding the first plateau. The potential region for the $SbPO_4$ system is close to that for Sb_2O_3 and Sb_2O_4 systems; also, its higher voltage may be due to the low lattice energy of $SbPO_4$ (1415 kcal/mol) relative to Sb_2O_3 (4844 kcal/mol). These values were obtained from

Table 1
Electrochemical characteristics of the first discharge curve for the $Li/LiPF_6$(EC, DEC)/$SbPO_4$ cell at different discharge rates (x is expressed as the $Li/SbPO_4$ mole ratio)

Galvanostatic regime	1st plateau	2nd plateau	Total lithium uptake
$C/5$	$0.0<x<2.3$	$3.1<x<4.2$	4.8
$C/10$	$0.0<x<2.4$	$3.2<x<4.8$	5.8
$C/20$	$0.0<x<2.6$	$3.5<x<6.2$	7.0

the Kapustinkii equation, using the thermochemical radius for PO_4^{3-} ion [22].

The extent of the first plateau suggests complete dissociation of the phosphate according to

$$SbPO_4 + 3\ Li \rightarrow Sb + Li_3PO_4. \quad (4)$$

Therefore the reaction between lithium and $SbPO_4$, is not an intercalation reaction, but one that destroys the network. In fact, other layered phosphates such as SnP_2O_7 [7], $SnHPO_4$ [8] and $Pb_3(PO_4)_2$ [9] are decomposed by lithium, this latter according to (1). A potential initial occupancy by lithium ions of interstitial sites defined in the interlayer spacing of these three compounds has not yet been considered. However, Behm and Irvine [7] have postulated that, although tin phosphate structures are destroyed in the first plateau, the structure of the resulting products is closely related to that of the pristine materials. In support of this statement is the strong dependence between the electrochemical reaction with lithium and the crystal structure of the two polymorphs of SnP_2O_7 (cubic or layered). This suggests that the layered character of the pristine material is not a negligible factor. Moreover, if the reaction occurred via an intercalation mechanism, one could expect it to be reversible reaction; however the CVs of Fig. 4a are consistent with the mechanism of reaction (4). The plateau width approaches the stoichiometric value as the discharge rate decreases (see Table 1).

The origin of the second plateau in the discharge curves of Fig. 4 can be analyzed by comparison with that reported for other antimony-based compounds. One domain at 0.8 V is commonly observed in the formation of lithium–antimony alloys from antimony-based systems, as antimony [23], intermetallics [24,25] or oxides [20,21]. Antimony particles formed during the first plateau can further react with lithium to yield Li_2Sb or Li_3Sb according to

$$Sb + 2\ Li \rightarrow Li_2Sb. \quad (5)$$

or

$$Sb + 3\ Li \rightarrow Li_3Sb. \quad (6)$$

However, Li_2Sb is often assumed to be virtually undetectable as it reacts very rapidly with lithium [23,24]:

$$Li_2Sb + Li \rightarrow Li_3Sb. \quad (7)$$

For the faster discharges ($C/5$ and $C/10$), the second plateau corresponds to 1.1 and 1.6 mol of Li, respectively, which means that not all of the antimony particles formed in the electrode are transformed into Li_3Sb (see Table 1). However, the experimental uptake of lithium for the slow discharge at $C/20$, 2.7 mol, is close to the theoretical value. Therefore, the current density strongly affects the kinetics of the process, the effect being related to the growth of lithium–antimony alloys from antimony nuclei formed during the first plateau.

With the aim of confirming the previous mechanism for reaction with Li, ex situ X-ray diffraction patterns were recorded for the electrode upon discharge at a depth of 3.0 or 6.0 Li atoms per mole of compound. Unfortunately, the resolution of the XRD patterns (Figs. 1b and c) was too low to allow the reflections corresponding to the new phases to be clearly distinguished. Nevertheless, they allow some conclusions to be drawn, namely: (i) the electrochemical reaction results in dramatic amorphization of the material; (ii) Li_3PO_4 phase, which is poorly crystalline, appears when the electrode is discharged—which validates reaction (4); and (iii) the main reflections observed for the pattern at $x = 3.0$ correspond to the pristine phase—which indicates that reaction (4) is incomplete.

Additional information is also supplied by the morphology of the electrode particles at different depths of discharge. Upon reaction with lithium, the electrode is composed of agglomerates of round particles (Fig. 5a) due to both the composite nature of the electrode and, according to reaction (4), the destruction of $SbPO_4$. A drastic volume change should occur in the electrode when antimony is lithiated to yield the lithium richest phase ($V[Li_3Sb]/V[Sb] = 3.23$). This suggests that the electrode particles must expand during reaction (6), thereby causing the particles to disconnect from one another and from the current collector. A higher current density would favour the transition $Sb \rightarrow Li_3Sb$ in some antimony nuclei rather than the homogeneous formation of Li_2Sb (and later Li_3Sb), in the whole electrode. This also explains why a lower discharge rate can supply a better electrochemical response: the formation of the Li_3Sb phase involves practically the widely distributed antimony nuclei produced along the first plateau. This mechanism is supported by the SEM images of different sections of the electrode stopped at $x = 6.6$ (Figs. 5b and c). The interparticles connection has decreased and the average particle size is greater than in the previous steps. A similar expansion has been observed in deeply discharged germania electrodes [26] and tin oxide thin films [14].

Complementary information was obtained by analysing the voltage tail at the end of the discharge curve (Fig. 4). This has also been observed in other antimony compounds and associated to the development of a solid electrolyte interface (SEI) at low voltages or the inclusion of lithium in the antimony or carbonaceous particles constituting the electrode [27–29]. Recently, Dailly et al. postulated that both the formation of an SEI and the alloying of Sb with further lithium occur simultaneously over the 0.8–0.5 V range [28]. The SEI, in addition to its insulating layer behavior, also contributes to the disconnection between electrode particles and, together with the volume expansion caused by the

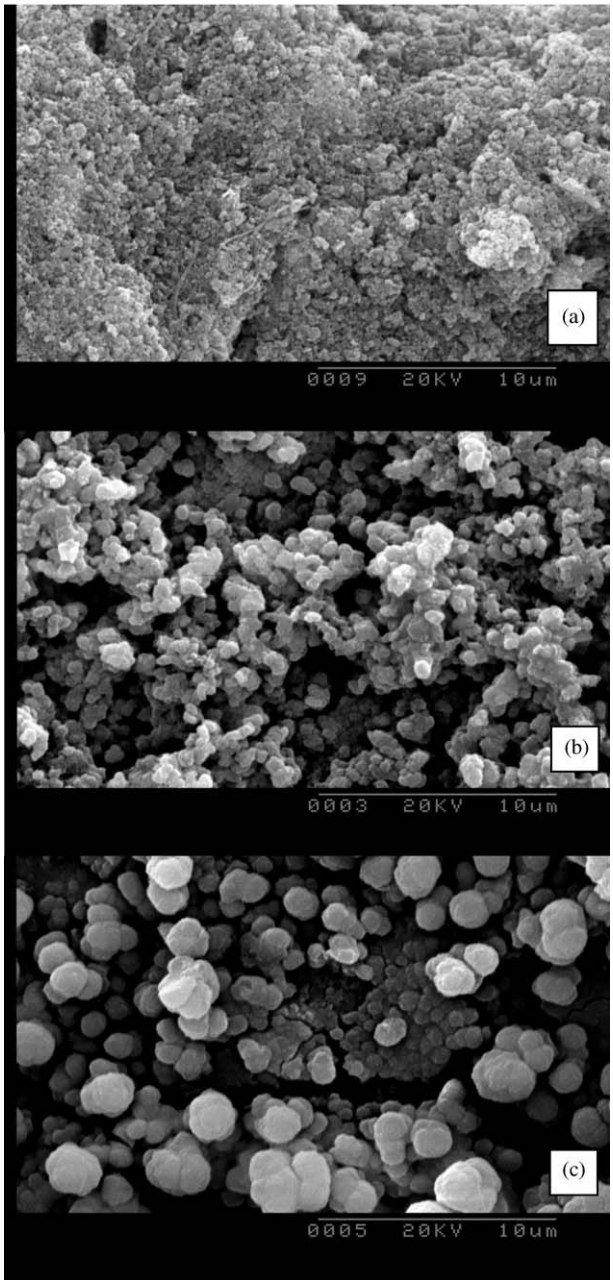

Fig. 5. Scanning electron micrographs of $SbPO_4$ subjected to variable discharge depths: (a) $x = 2.0$, (b) and (c) $x = 6.6$. Discharge rate $C/20$.

alloying of antimony, accounts for the volume increase at the electrode (Figs. 5b and c).

The evidence for the presence of the SEI film is supported by the presence of the two cathodic peaks at a 0.13 V and near zero volts in the CV curves (Fig. 3b). When the cell is charged, two other peaks appear at 0.17 and 0.24 V which suggest that the electrochemical reaction is reversible. Dissolution of the SEI during the charge process has also been reported for some transition metal oxides such as CoO [30], but was found to be strongly dependent on the particular voltage range. Moreover, the formation of the SEI at the surface of lithium storage metals such as tin or antimony is detrimental [27] as its potential dissolution during the charge process will expose fresh metal surface and more film will be formed in the next discharge. Therefore, further cycling can lead to an increasing number of disconnected electrode particles. For this reason, Besenhard et al. [27] have proposed the use of surfactants to hinder formation of the passive film.

The electrochemical performance of the $Li/LiPF_6$(EC, DEC)/$SbPO_4$ cell was studied in different cycling tests. Provision was made for the combined effect of Li_3Sb at the end of the discharge and for the presence of the SEI layer, which promoted crumbling of the electrode material. Thus, a lower cut-off voltage, 0.25 V, was used with the aim of lessening detrimental effect of the SEI film on the aggregation of the electrode particles. Figs. 6a and b show the galvanostatic cycles following the first discharge under different current regimes ($C/20$ and $C/10$) and voltage ranges (2.0–0.25 V and 1.25–0.25 V, respectively). In both cases, the formation of Li–Sb alloys occurred at 0.7 V and was signalled by a *pseudoplateau*. Such a plateau was long over the 2.0–0.25 V voltage range, and three Li^+ ions per mole of $SbPO_4$ were reversibly consumed in the first cycle, consistent with reactions (5)–(7). The curve length was dramatically shortened for the cell cycled over the

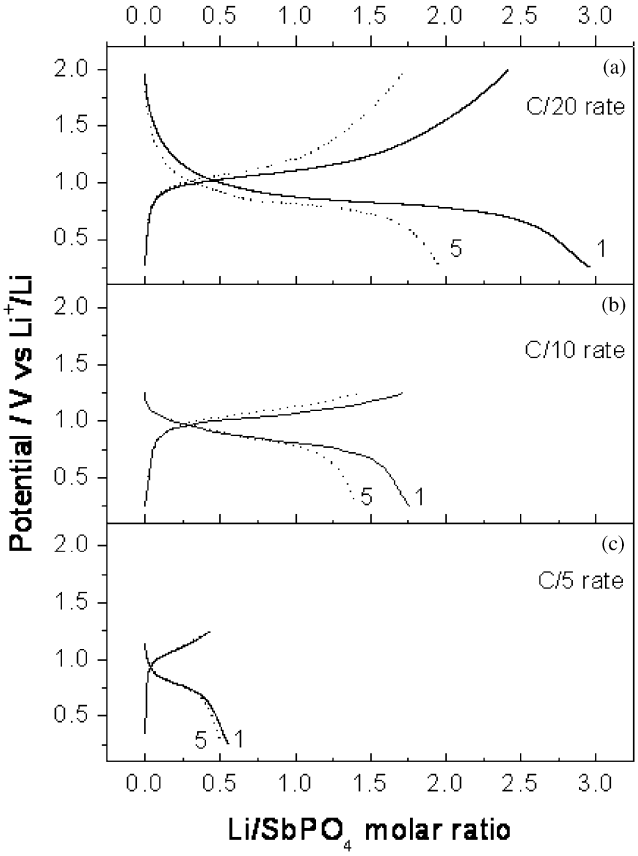

Fig. 6. (a–c) Selected galvanostatic cycles of the $Li/LiPF_6$(EC, DEC)/$SbPO_4$ cell under various regimes and voltage ranges.

1.25–0.25 V range and submitted to a faster discharge, $C/10$. However, it is noteworthy that, under these conditions, a lower capacity loss was observed at the fifth cycle relative to the 2.0–0.25 V range. This clearly reveals that the $Li_2Sb + Li \rightarrow Li_3Sb$ reaction is more efficient than the $Sb + 2Li \rightarrow Li_2Sb$ and/or $Sb + 3Li \rightarrow Li_3Sb$ reaction, which has been shown to be reversible for various antimony-based electrodes consisting of InSb [25], Sb_2O_x [20,21] and Zn_4Sb_3 [31]. The extent to which the cell is polarized is strongly dependent on the applied current density; thus, the electrochemical response worsens under the $C/5$ galvanostatic regime (Fig. 6c). From these results we can conclude that the growth of the Li_3Sb alloys modulates the electrode behavior, as we discussed in the SEM section.

Fig. 7 shows the specific capacity delivered by the cells on cycling. The cell cycled over the 2.0–0.25 V range exhibited a significant fade in capacity down to a constant value of 150 A h kg^{-1} at the 40th cycle (40% of that delivered in the first cycle). Conversely, the capacity of the cells cycled over the 1.25–0.25 V range faded gradually, which confirms the good reversibility of reaction (7). Both results can be ascribed to the loss of contact between particles promoted by the volume changes during the formation of different Li–Sb alloys along the second plateau. However, not only this factor must be considered, when compared with cervantite (Sb_2O_4) thin films [21]. Over this voltage range, these films exhibit a high capacity retention (340 A h kg^{-1} at 50th cycle). One important difference between the two discharged systems ($SbPO_4$ and Sb_2O_4) is the lithium compound formed during reaction (4) or (3), respectively. If we assume this lithium compound to surround the antimony particles formed, their electrochemical activity must be obviously affected. Li_3PO_4 behaves as a poorly conductive matrix [4], whereas Li_2O is an ionic conductor [5,6,14]. This factor is seemingly very important in explaining a view the capacity retention of these antimony systems.

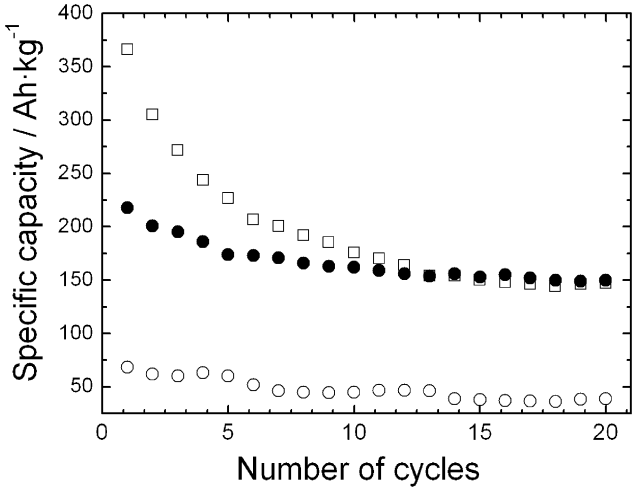

Fig. 7. Capacity versus cycle number plot for the Li/$LiPF_6$(EC, DEC)/$SbPO_4$ cell at different voltage ranges and galvanostatic regimes: (□) 2.0–0.25 V and $C/20$; (•) 1.25–0.25 V and $C/20$; (○) 1.25–0.25 V and $C/5$.

The best results for the antimony phosphate cells were those obtained by cycling at $C/20$ over the 1.25–0.25 V range, where an average 165 A h kg^{-1} (264 A h/kg of Sb, 75% of the energy delivered in the first cycle) was maintained over the first 20 cycles. The electrochemical properties exhibited by the electrode are better than those reported for other metallic phosphates such as $SnHPO_4$ [8] or $Sn_2P_2O_7$ [32] used as anode materials, in terms of delivered energy and capacity loss. However, they are worse than those reported for cubic SnP_2O_7 [7], with 270 Ah kg^{-1} at the 100th cycle. Interestingly, possibly connected with our layered antimony phosphate, the layered polymorph of tin pyrophosphate exhibits poorer capacity retention than the cubic polymorph [7]. In spite of the good cycling properties exhibited by our electrode, the total energy delivered is too low to consider the potential use of this material for anodes in lithium batteries. New efforts must be with a view to improving the electrochemical properties of the $SbPO_4$ compound. In this respect, the influence of the morphology of the pristine compound and the reversibility of $Sb \rightarrow Li_xSb$ reaction on electrochemical performance will be addressed in future work.

4. Conclusions

Antimony orthophosphate, $SbPO_4$, is a layered phosphate that possesses a rich intercalation chemistry towards different organic molecules. In this work, we have examined the electrochemical reactivity of $SbPO_4$ towards lithium by means of cyclic voltammetry and galvanostatic measurements applied to cells of the Li/$LiPF_6$(EC, DEC)/$SbPO_4$ type. Two different voltage ranges were examined with a view to assess its potential as a material for positive or negative electrodes in these cells. The irreversibility of the reaction over 2.0–1.2 V range excludes its use as a positive electrode. By contrast, the electrochemical processes that occur over the 2.0–0.0 V range are reversible and, at moderate discharge rates, the compound exhibits a good capacity retention with cycling. Thus, the material has the potential for use as a negative electrode; however, its main drawback (viz. the fairly low capacity it delivers) requires that the resulting electrode be optimized.

Acknowledgments

This work was funded by Junta de Andalucía (Group FQM-175) and Spain's Ministry of Science and Technology (Project MAT2002-04477-C02-02).

The authors also wish to acknowledge Dr. Fernando Hierro, from Serveis Cientifics of UIB, for his help in obtaining the SEM and TEM images.

References

[1] K. Mizushima, P.C. Jones, P.J. Wiseman, J.B. Goodenough, Mater. Res. Bull. 15 (1980) 783.
[2] J.R. Dahn, U.V. Sacken, M.W. Juzkov, H. Aljanaby, J. Electrochem. Soc. 138 (1991) 2207.
[3] T. Ohzuku, in: G. Pistoia (Ed.), Lithium Batteries, Elsevier, Ámsterdam, 1994, p. 239 (Chapter 6).
[4] T. Ohzuku, Y. Makimura, Chem. Lett. (2001) 744.
[5] Y. Idota, M. Nishima, Y. Miyaki, T. Kubota, T. Miyasaki, Canada Patent Appl. 2.134.053 (1994).
[6] I.A. Courtney, J.R. Dahn, J. Electrochem. Soc. 144 (1997) 2045.
[7] M. Behm, J.T.S. Irvine, Electrochim. Acta 47 (2002) 1727.
[8] M.L. Elidrissi Moubtassim, J.I. Corredor, J.M. Lloris, C. Pérez Vicente, J.L. Tirado, J. Electrochem. Soc. 149 (2002) A1030.
[9] Z. Liu, J.Y. Lee, J. Power Sources 97–98 (2001) 247.
[10] I. Sandu, T. Brousse, J. Santos-Peña, M. Danot, D.M. Schleich, Ionics 8 (2002) 270.
[11] M. Martos, J. Morales, L. Sánchez, Electrochim Acta 48 (2003) 615, 6.
[12] M. Martos, J. Morales, L. Sánchez, J. Mater Chem. 12 (2002) 2979.
[13] J. Santos, T. Brousse, L. Sánchez, J. Morales, D.M. Schleich, J. Power Sources 97–98 (2001) 232.
[14] T. Brousse, R. Retoux, U. Herterich, D.M. Schleich, J. Electrochem. Soc. 145 (1998) 1.
[15] B. Kinberger, Acta Chem. Scand. 24 (1970) 320.
[16] H. Saadaoui, A. Bouchari, S. Flandrois, J. Aristides, Mol. Cryst. Liq. Cryst. 224 (1994) 173.
[17] V. Sudarsan, K.P. Muthe, J.C. Vyas, S.K. Kulshreshtha, J. Alloy Compound 336 (2002) 119.
[18] G. Alonzo, N. Bertazzi, P. Galli, M.A. Massucci, P. Patronp, F. Saiano, Mater. Res. Bull. 33 (8) (1998) 1221.
[19] W. Brockner, L.P. Hoyer, Spectrochim. Acta A 58 (2002) 1911.
[20] H. Li, X. Huang, L. Chen, Solid State Ionics 123 (1999) 189.
[21] J. Santos-Peña, J.J. Cuart-Pascual, I. Sandu, D.M. Schleich, T. Brousse in "New Trends in Intercalation Compounds for Energy Storage Conversion", C. Julien, K. Zaghib, Ed., the Electrochemical Society Proceedings Series, Pennington, NJ (2003).
[22] J. E. Huhey, in: Inorganic Chemistry, Principles of Structure and Reactivity, 2nd Ed., Harper and Row, New York, 1978, p. 51 (Chapter 3).
[23] R.A. Huggins, J. Power Sources 26 (1989) 109.
[24] J. Yang, M. Wachtler, M. Winter, J.O. Besenhard, Electrochem. Solid-State Lett. 2 (1999) 161.
[25] J.T. Vaughey, J. O'hara, M.M. Thackeray, Electrochem. Solid State Lett. 3 (2000) 13.
[26] J. Santos-Peña, I. Sandu, O. Joubert, F. Sánchez-Pascual, C. Otero-Areán, T. Brousse, Electrochem and Solid State Letters, in press.
[27] M. Wachtler, J.O. Besenhard, M. Winter, J. Power Sources 94 (2001) 189.
[28] A. Dailly, J. Ghanbaja, P. Willmann, D. Billaud, Electrochim. Acta 48 (2003) 977.
[29] D. Aurbach, Y. Ein-Eli, A. Chusid, Y. Carmeli, Y. Babori, H. Yawh, J. Electrochem. Soc. 141 (1994) 603.
[30] S. Laruelle, S. Grugeon, P. Poizot, M. Dollé, L. Dupont, J.M. Tarascon, J. Electrochem. Soc. 149 (5) (2002) A627.
[31] X.B. Zhao, G.S. Cao, Electrochim. Acta 46 (2001) 891.
[32] Y.W. Xiao, J.Y. Lee, A.S. Yu, Z.L. Liu, J. Electrochem. Soc. 146 (1999) 3623;
J.Y. Lee, Y. Xiao, Z. Liu, Solid State Ionics 133 (2000) 25.